HHS Public Access

Author manuscript

Annu Rev Anal Chem (Palo Alto Calif). Author manuscript; available in PMC 2016 May 04.

Published in final edited form as:

Annu Rev Anal Chem (Palo Alto Calif). 2015 ; 8: 239–261. doi:10.1146/annurev-anchem-071114-040426.

Electrochemical Analysis of Neurotransmitters

Elizabeth S. Bucher and **R. Mark Wightman**

Department of Chemistry and Neuroscience Center, University of North Carolina at Chapel Hill, Chapel Hill, North Carolina 27599

Elizabeth S. Bucher: ebucher@email.unc.edu; R. Mark Wightman: rmw@unc.edu

Abstract

Chemical signaling through the release of neurotransmitters into the extracellular space is the primary means of communication between neurons. More than four decades ago, Ralph Adams and his colleagues realized the utility of electrochemical methods for the study of easily oxidizable neurotransmitters, such as dopamine, norepinephrine, and serotonin and their metabolites. Today, electrochemical techniques are frequently coupled to microelectrodes to enable spatially resolved recordings of rapid neurotransmitter dynamics in a variety of biological preparations spanning from single cells to the intact brain of behaving animals. In this review, we provide a basic overview of the principles underlying constant-potential amperometry and fast-scan cyclic voltammetry, the most commonly employed electrochemical techniques, and the general application of these methods to the study of neurotransmission. We thereafter discuss several recent developments in sensor design and experimental methodology that are challenging the current limitations defining the application of electrochemical methods to neurotransmitter measurements.

Keywords

amperometry; voltammetry; carbon-fiber microelectrodes; biosensors; catecholamines; exocytosis

1. INTRODUCTION

Brain neuronal communication primarily occurs through the exocytotic release of neurotransmitters into synaptic junctions and the surrounding extracellular fluid. These chemical signaling molecules modulate postsynaptic cell activity in various ways dependent on the identity of the neurotransmitter and the receptors that are recruited. The downstream effects of neurotransmission underlie a wide range of physiological and behavioral processes and its dysregulation can lead to a number of debilitating disorders as broad as Parkinson's disease, Alzheimer's disease, depression, and drug addiction (1–4).

Errata

An online log of corrections to *Annual Review of Analytical Chemistry* articles may be found at http://www.annualreviews.org/errata/anchem

DISCLOSURE STATEMENT

The authors are not aware of any affiliations, memberships, funding, or financial holdings that might be perceived as affecting the objectivity of this review.

Before the 1970s, radioimmunoassays were the only available technique with the requisite sensitivity to detect the small chemical concentrations produced by neurotransmission (5). During the latter part of the 1960s, however, Ralph Adams and his colleagues studied the electrochemistry of a number of easily oxidizable biogenic amines and quickly realized the potential applications of their knowledge to the field of neurochemistry. Shortly thereafter, Adams implanted a carbon-paste electrode into the brain of an anesthetized rat and, quite boldly, demonstrated that traditional voltammetric techniques could be applied successfully to biological tissues (6). Even though the signal recorded was likely ascorbic acid and not dopamine as had been hoped, this work importantly suggested that neurotransmitters could escape the confined space of the synaptic cleft and diffuse to the electrode surface—without which in vivo electrochemical measurements would be impossible.

The early days of in vivo electrochemistry were fraught with issues of selectivity, mainly due to interference from catecholamine metabolites and ascorbic acid (7). However, over the past four decades, numerous methods have been developed not only to increase the selectivity of these measurements, but also to apply them at subsecond timescales. As Adams had envisioned, in vivo electrochemistry now encompasses a matured set of techniques employed by countless neuro-science and psychology laboratories to study the release, uptake, and signaling dynamics of rapid neurotransmission. Electrochemical techniques have been used in a wide variety of applications, ranging from resolution of single exocytotic events from single cells to monitoring of neurochemical fluctuations in awake, behaving animals.

It is impossible to cover the entire scope of electrochemical detection of neurotransmitters in a single review. This review, therefore, has two goals. First, we provide a general understanding of common electrochemical techniques used for neurotransmitter detection. Second, we highlight several new applications defining the next generation of in vivo electrochemical research.

2. DETECTION OF NEUROTRANSMITTERS WITH ELECTROCHEMICAL TECHNIQUES

To monitor neurotransmitter fluctuations in living tissues, researchers have applied several different electrochemical techniques including amperometry, various potential pulse methods, and cyclic voltammetry (7–9). In general, these methods detect target neurotransmitters through their oxidation or reduction at a solid electrode. The currents generated provide a quantitative measure of dynamic chemical fluctuations that can be correlated to pharmacology, behavior, and disease pathology. Target molecules are limited to those that are electroactive within the potential window of the interstitial fluid; these include the biogenic amines (dopamine, norepinephrine, and serotonin), their metabolites, and ascorbic acid. Here we briefly overview the most common techniques in current use.

2.1. Constant-Potential Amperometry

In constant-potential amperometry, often referred to simply as amperometry, the electrode is held at a potential sufficient to oxidize or reduce an analyte of interest so that the currents

generated are mass transport limited. As the potential is constant throughout the duration of the experiment, no charging currents are generated and direct integration of the currents detected provides the amount of analyte electrolyzed according to Faraday's law ($Q = nNF$). Moreover, the time resolution of the experiments is limited only by the data acquisition rate. However, these measurements provide very little chemical information, as any molecule that is electroactive at a given potential will be detected and should be applied only to samples of known content. For example, ex situ analyses typically preprocess samples through separation methods, such as liquid chromatography. Indeed, liquid chromatography with amperometric detection was one of the first viable methods for brain tissue content analysis (5) and is still in common use today.

Cell cultures are typically relatively homogenous in their chemical composition, and their contents can be predetermined by other analyses, making them suitable for amperometric analysis (10). Intracellular communication occurs through exocytosis, by which a neurotransmitter-filled vesicle docks and fuses to the cell membrane and releases its contents into the extracellular space. The high temporal resolution of amperometry is useful for the study of exocytosis of monoamines from single cells and cell cultures. In such experiments, a small beveled disk electrode is placed near the cell membrane. Chemical stimulation of the cell is used to evoke neurochemical release. Single exocytosis events are resolved as millisecond-wide spikes in oxidative current. Whereas integration of the current response gives the moles of neurotransmitter released, additional quantitative and qualitative information can be determined from the shape of the spike. The peak's rise time (10–90%) correlates to the opening kinetics of the fusion pore between the cell membrane and the neurotransmitter-filled vesicle. The spike's half-width indicates the duration of the release event. The recently discovered presence of post–spike plateau currents is indicative of partial-fusion, or kiss and run, events (11). Amperometric measurements have been applied to a variety of cell types including adrenal chromaffin cells (12), pheochromocytoma (PC12) cells (13), mast cells (14), and neurons (15, 16) to probe the pharmacology and biophysics of vesicular release events.

2.2. Fast-Scan Cyclic Voltammetry

In fast-scan cyclic voltammetry (FSCV), a triangular waveform is applied to a microelectrode at a high scan rate (>100 V/s) to rapidly oxidize and reduce electroactive species at the electrode surface. Various performance aspects (i.e., sensitivity, selectivity, and temporal resolution) can be optimized by altering the potential limits, scan rate, and application frequency of the waveform. For instance, a commonly used dopamine waveform scans from −0.4 V to +1.3 V at 400 V/s, repeated at 100-ms intervals. The rapid scan generates a large background current that arises mainly from the charging of the electrical double layer and is proportional to the capacitance of the electrode. Thus, to resolve the smaller faradaic currents the background current is subtracted, usually by digital means. In the resulting cyclic voltammogram, the peak potentials provide a chemical signature to identify the species detected. Peak currents are usually converted into concentrations using calibration factors obtained from standards of known concentration.

Given its chemical selectivity, FSCV has been widely employed in vitro and in vivo to detect a number of electroactive species including but not limited to dopamine, norepinephrine, serotonin, O_2, and pH changes (17–19). Many FSCV studies use electrical stimulation to elicit monoamine release in terminal regions. The rising phase of these responses is determined by release (modified by its autoinhibition) and uptake mechanisms, whereas the falling phase is principally governed by uptake. Both phases are convoluted with diffusion from the site of release to the electrode. Thus, measurement of these parameters can be used to assay the function of these regulatory mechanisms (20–22).

Of the biogenic amines, dopamine is the most common target of FSCV measurements. Studies in brain slices and anesthetized animals have proven particularly useful in delineating the regulatory mechanisms controlling dopamine release and uptake in subregions of the striatum and how these processes are disturbed in disease states (23–26). The use of voltammetry in freely moving animals has been a major accomplishment that has contributed much to our understanding of the central dopamine system and how it drives motivated behaviors during reward-based learning (27, 28) and drug addiction (29–31). In contrast, application of FSCV to the detection of norepinephrine and serotonin in vivo has only recently been possible owing to issues of selectivity and electrode fouling, respectively. To overcome these challenges, researchers have identified several strategies involving anatomical positioning for norepinephrine and waveform/electrode modifications for serotonin. Subsequent work has successfully investigated the regulation of norepinephrine overflow in the bed nucleus of the stria terminalis (32, 33) and serotonin overflow in the substantia nigra pars reticulata (34, 35).

3. ELECTROCHEMICAL DETECTION OF NEW NEUROMODULATORS

Investigators have made several attempts to extend the high temporospatial resolution of in vivo electrochemical detection to target molecules that are more difficult to electrolyze. These efforts have principally used two approaches. In one, the electrode is modified with an enzyme selective for the molecule of interest. In the other, the parameters of the applied voltage sweep have been adjusted. These strategies are discussed in more detail below.

3.1. Enzyme-Modified Electrodes

Enzyme-modified electrodes can detect a range of nonelectroactive species in biological tissue. In such measurements, an enzyme with specific activity for an analyte of interest is immobilized to the electrode surface covalently or through film coating. The activity, stability, and selectivity of the enzyme in its immobilized form are crucial aspects of sensor performance (36). Analyte detection is accomplished through the formation of an electroactive product, often H_2O_2 formed by an oxidase. For instance, the detection of glutamate, the principal excitatory neurotransmitter, can be achieved with glutamate oxidase, which converts glutamate into α-ketoglutarate and H_2O_2 (37). A secondary enzyme-free electrode is often required to account for nonspecific currents (38). As the kinetics of the enzyme can slow the temporal resolution of such measurements, enzyme-based sensors are usually coupled to amperometry. Amperometric enzyme sensors have been developed for many nonelectroactive neurotransmitters, including glutamate (37, 39), acetylcholine (40) and its precursor choline (41), and adenosine (42).

The chemical information provided by FSCV can alleviate many of the selectivity issues experienced with enzyme-based amperometric sensors. In the past, the use of enzyme-based detection schemes with FSCV at carbon-fiber microelectrodes has largely been limited by the slow electron-transfer kinetics of H_2O_2. However, Sanford et al. (43) recently demonstrated that overoxidizing the carbon-fiber surface with an extended +1.4 V anodic scan facilitates the oxidation of H_2O_2 with FSCV. Because the overoxidation process occurs near the anodic switching potential with this extended waveform, the oxidation peak for H_2O_2 appears at +1.2 V on the reverse scan. To detect glucose with this waveform, carbon-fiber microelectrodes were coated by electrodeposition of glucose-oxidase in chitosan, a nontoxic polysaccharide (44). This sensor has a 13-μM limit of detection for glucose; stable performance over a 4-h period; and the ability to discriminate against interferents such as dopamine, ascorbic acid, and pH. This work establishes the utility of enzyme-based FSCV sensors for the detection of nonelectroactive species.

3.2. Waveform Modification Strategies

Many brain molecules are electroactive but are not oxidized by the voltammetric sweep employed for dopamine measurements (−0.4 V to +1.3 V, 400 V/s). Several of these molecules can be detected by modifying the anodic limits of the potential scan to promote electron transfer. For example, adenosine, which is formed from the degradation of ATP, is a purine signaling molecule that regulates cerebral blood flow, metabolism, and the activity of different neurotransmitters (45). Detection of adenosine is accomplished by increasing the anodic limits of the traditional dopamine waveform to +1.5 V (46). This generates an initial oxidation peak at the anodic switching potential and a second oxidation peak at +1.0 V on the forward scan. The second oxidation peak arises from sequential oxidation of the initial electroformed product. Both of these oxidation processes are irreversible; hence, no reduction peaks are generated. Since its development, this modified waveform has been used to monitor adenosine dynamics in preparations as varied as murine spinal lamina (47, 48), brain slices (49, 50), and the striatum of anesthetized rats (51). Initial results have found that adenosine release is evoked by mechanical stimulation (52) and correlates to local O_2 fluctuations in intact tissue (51). More recently, researchers have developed a “sawhorse” waveform that holds at 1.35 V for 1 ms during the anodic scan (53). The sawhorse waveform provides discrimination between adenosine and two major interferents, H_2O_2 and ATP, that oxidize at similar potentials, and may prove useful for in vivo experiments. In parallel studies, Schmitt et al. (42) used an enzyme-modified electrode to probe the dynamics of adenosine and its precursors.

Waveform strategies have also been incorporated to target various peptide neurotransmitters. Glanowska et al. (54) detected gonadotropin-releasing hormone (GnRH) release in mouse brain slices, where it plays a major role in fertility (55) and may act as a neuromodulator (56). GnRH was detectable because it contains the electroactive amino acid tryptophan. Although the oxidation of tryptophan can foul the electrode, stable oxidation currents were obtained for GnRH using a triangular waveform scanning from 0.5 V to 1.45 V at 400 V/s. With this waveform, the oxidation peak for GnRH occurs at ~1.25 V and could be distinguished from tryptophan and another tryptophan-containing peptide, kisspeptin-10. Measurements in brain slices revealed that GnRH release could be chemically evoked in the

median eminence and the preoptic area. No signal was detected from mice genetically modified to lack GnRH, thereby supporting its detection in wild-type animals.

FSCV has also been applied to the detection of the small opioid peptide, methionine-enkephalin (M-ENK) (57). M-ENK and other opioid peptides are involved with many physiological and behavioral processes, including reward processing, drug addiction, and pain perception (58). The electroactive moiety in M-ENK is tyrosine, which, similar to tryptophan, can cause electrode fouling. Schmidt et al. (57) demonstrated that M-ENK could be detected reproducibly and selectively with a variant of the sawhorse waveform that varied the scan rate on the anodic sweep. The optimized waveform scanned from −0.2 V to +0.6 V at 100 V/s, then to +1.2 V at 400 V/s. This anodic limit was held for 3 ms before scanning back to the −0.2 V holding potential at 100 V/s. The oxidation peak for M-ENK occurs at +1.0 V on this waveform, which exhibits selectivity against other tyrosine-containing peptides. As the oxidation peaks for catecholamines occur at more negative potentials, this waveform can be used to monitor simultaneous norepinephrine and M-ENK release from tissue extracted from the rat adrenal gland.

4. MICROSENSOR DEVELOPMENTS

The need for a miniaturized working electrode compatible with tissue implantation was recognized soon after the advent of in vivo electrochemistry (5). Smaller electrodes allow for minimal tissue damage, high spatial resolution to probe discrete brain regions, and faster sampling rates owing to their reduced RC properties. Given its low cost, good electrochemical properties, and biological compatibility, carbon was the intuitive choice for electrode material; however, the conventional carbon-paste electrodes of the 1970s were not amenable to miniaturization (59). In the late 1970s, Ponchon et al. (60) advanced the field of in vivo electrochemistry by introducing the carbon-fiber microelectrode. These electrodes are fabricated by sealing the carbon fiber (5–35 μm in diameter) in glass and either cutting the protruding fiber to form a cylindrical electrode or treating the seal with epoxy and polishing the tip to form an elliptical surface. Given the ease and reproducibility of their fabrication, carbon-fiber microelectrodes are routinely used in most in vivo electrochemical studies today (61).

Over the past several decades, various efforts have employed multiple methods to improve the performance of in vivo electrochemical sensors. For instance, researchers have investigated surface-modification techniques to enhance the selectivity, sensitivity, and kinetic properties of carbon-fiber microelectrodes. Broadly speaking, these techniques have included electrochemical (62) and chemical (63) pretreatments as well as film coating. Application of the perfluorinated cation-exchange polymer Nafion through electrodeposition or dip coating has proven particularly effective in repelling negatively charged interferents during in vivo measurements (35). Below we highlight several more recent developments in in vivo electrochemical sensor technology.

4.1. Carbon-Nanotube-Based Microelectrodes

Given their mechanical strength, high aspect ratios, and good electrical conductivities, carbon nanotubes (CNTs) have been explored for various electrochemical applications (64,

65). Research exploring modification of carbon-fiber microelectrodes with CNTs for neurotransmitter measurements has shown increased electron-transfer kinetics and sensitivity for adsorption-controlled species such as dopamine. Such electrodes are also less susceptible to common biofouling agents, such as 5-HIAA. Immobilization of CNTs onto carbon-fiber microelectrodes was first achieved by dip-coating the fibers in a CNT-Nafion suspension (66). However, this method was found to suffer from poor reproducibility and the orientation of the CNTs restricted access to electroactive sites at the ends of the tubes. Further work identified chemical self-assembly of single-walled CNTs to be an effective method to form uniformly aligned CNT layers on carbon-fiber disk electrodes (67). Application of these CNT-modified electrodes in vivo and in vitro demonstrated a 36-fold increase in sensitivity for dopamine without decreasing response time, a problem that often occurs with other pretreatment methods.

Continuous fibers, or yarns, can be formed from CNTs via liquid-state and dry-state spinning methods (68, 69). By adjusting the size of the nanotubes and the spinning angle, yarns with diameters on the micrometer scale can be prepared. Disk microelectrodes (5–30 μm in diameter) fabricated from multiwalled CNT yarns exhibit a number of interesting electrochemical properties including lower background currents and faster apparent electron-transfer kinetics, which allows enhanced chemical discrimination (Figure 1) (70, 71). Although the time spent at negative holding potentials is a critical factor determining the sensitivity to dopamine at bare electrodes, the dopamine response at yarn microelectrodes is independent of the waveform application frequency—believed to be due to slower desorption kinetics for dopamine-*o*-quinone. Jacobs et al. (70) demonstrated that dopamine could be detected at a 2-ms timescale while maintaining sensitivity, simply by increasing the scan rate and application frequency of the waveform. Other work found that sensitivity for dopamine is enhanced even further when the yarns are made in polyethyleneimine, instead of poly(vinyl alcohol) (72). Together, these findings indicate that CNT-based microelectrodes provide sensitive, selective FSCV measurements at unprecedented speeds. However, it is not yet clear whether the significance of these advantages is sufficient to result in the widespread use of CNT microelectrodes.

4.2. Fused-Silica Carbon-Fiber Microelectrodes

Traditionally, carbon-fiber microelectrodes are insulated within borosilicate glass capillaries. Though easy to fabricate, glass-sealed microelectrodes are fragile and often break during routine experimental procedures. For more robust electrode construction, several groups have investigated the use of fused-silica capillaries (73–75). Fused silica offers good insulating properties and increased flexibility at low cost. During fabrication, an epoxy droplet is used to form a seal at the carbon fiber. As fused silica is less prone to breakage, smaller-diameter (100 μm versus 600 μm) electrodes are possible, which allows for less tissue damage during implantation.

Several years ago, Clark et al. (76) found that naturally evoked dopamine release could be measured at polyamide-coated fused-silica electrodes several months after in vivo implantation. Incredibly, measurements were obtainable for up to 25 successive days without any apparent loss in sensitivity—though there was a noted loss in temporal

response. Given the heterogeneity of brain microenvironments, the ability to conduct FSCV measurements from the same terminal population over multiple days is an exciting prospect for studies of disease and behavioral learning. Indeed, others have attempted to develop such a sensor (77, 78), albeit with little success. The performance of the fused-silica electrode design is attributed to its size, which may be small enough to bypass the immune response.

Questions as to how these sensors can be used remain. Although postcalibration of the sensors revealed no changes in electrode sensitivity after chronic implantation, it is unclear whether sensor performance remains stable after several days of in vivo use. Unforeseen issues such as new tissue damage or degradation of the carbon fiber could change the electrode's response with continued use. In such cases, it would be impossible to determine whether a signal decrease is a biologically relevant change or merely a change in electrode sensitivity. These concerns are the subject of ongoing studies.

4.3. Microelectrode Arrays

Neurotransmitter release varies not only within discrete substructures of the brain (79) but also across individual cells (80). This has spurred the development of microelectrode arrays (MEAs) compatible with neurochemical measurements for a variety of in vitro and in vivo purposes. Consolidation of multiple sensing elements onto a single device makes possible spatially resolved profiling of neurochemical dynamics as well as simultaneous detection of different analytes by optimizing the potentials applied to each electrode.

To capture exocytotic variation on a subcellular level, MEA size and electrode spacing must be smaller than the cell (~10–20 μm for a neuron). For single-cell measurements, carbon-disk MEAs have been fabricated from carbon fibers inserted into multibarrel glass and from the deposition of carbon through pyrolysis onto a fused assembly of quartz capillaries to form up to 7 and 15 electrodes, respectively (81, 82). Researchers have also employed various microfabrication approaches to create MEA devices with an increased electrode number for single-cell and cell-cluster applications (83–85). Recently, Ewing and coworkers (86, 87) developed platinum MEA platforms that are modified with collagen IV coatings to promote cell adhesion and growth. The newest version of their design confines 36 microelectrodes within a 40 μm × 40 μm microwell to position a cultured PC12 cell directly above the sensor surface.

Most MEAs developed for in vivo neurochemical applications have been carbon based given carbon's compatibility with FSCV. These arrays have been used to probe neurotransmitter heterogeneity across multiple brain regions and within brain microenvironments. In vivo recordings are possible by simply implanting several individual carbon-fiber microelectrodes (76, 88). However, such methodologies can suffer from irreproducibility and are difficult to implement when targeting a single brain structure. Hence, recent efforts have focused on the microfabrication of carbon-based MEAs. Successful devices containing 4- and 16-band microelectrodes have been created from pyrolyzed photoresist, which is amenable to photolithography and has properties similar to glassy carbon (89). Strategies to construct MEAs from grown carbon nanofibers are also under investigation, but the viability of such devices in vivo has yet to be demonstrated (90).

5. NOVEL APPLICATIONS

5.1. Challenging the Conventions of Neurochemical Measurements

Microdialysis and FSCV are the two most common in vivo neurochemical techniques in use today. Early in their development, microdialysis and FSCV were viewed as rival methods, but they are now recognized as providing complementary information. Millisecond temporal resolution makes FSCV superior for fast neurochemical measurement of electroactive molecules; however, the need for background subtraction limits detection to rapid concentration changes. With microdialysis, neurotransmitters and other small biomolecules in the brain extracellular fluid are extracted into dialysate driven slowly through a tubular semipermeable membrane. Because the dialysate is collected and analyzed externally in microdialysis, a wider range of molecules may be detected with better chemical selectivity. However, sampling times are typically on the order of minutes, the time required to collect sufficient dialysate for analysis. Here we describe several novel strategies that are currently being developed to redefine the current conventions of FSCV and microdialysis measurements.

5.1.1. Basal-level measurements with FSCV—Given dopamine's relevance to disorders such as Parkinson's disease, determining its basal level has been a goal of both microdialysis and FSCV. Because FSCV is a differential technique, it has required indirect approaches to approximate local extracellular concentrations. For instance, studies have employed pharmacological methods to rapidly silence dopamine signaling in the striatum (91–93). The subsequent decrease in extracellular dopamine detected at the electrode is assumed to represent the original baseline concentration. Others (8, 94) have used kinetic and diffusion modeling to extrapolate the basal level from the transient dopamine responses elicited by electrical stimulation. Although many of these studies predict the basal concentration of dopamine to be in the lower nanomolar range, others have reported values greater than 1 μM. Therefore, the results of these experiments remain the subject of debate.

Other measurement strategies have taken advantage of the predisposition of dopamine to adsorb to carbon-fiber surfaces via electrostatic and pi-pi stacking interactions (62, 95). These techniques use the signals generated after preconcentration of dopamine at the sensors as a measure of extracellular concentrations, similar to methods employed during anodic stripping voltammetry. One such approach involves a collector-generator-like system on a microfabricated platform (96). When operated, the potential of the outer-generator electrodes is held at = 0 V to promote the adsorption of dopamine and then pulsed to a positive potential to desorb the accumulated dopamine at the surface. This repulsion creates a transient wave of dopamine that is detected at the inner-collector electrode with FSCV and is used to determine the concentration of dopamine surrounding the device. Though detection of 200 nM dopamine was the lowest concentration demonstrated, the spacing of electrodes in future generations can be decreased for improved capture efficiency.

A similar approach has been developed for use with a single carbon-fiber microelectrode (97). In this technique, termed fast-scan controlled adsorption voltammetry (FSCAV), the holding time between voltammetric scans is altered to promote the adsorption of dopamine in a controlled manner. There are three steps to this process. First, a high-speed (1,200 V/s)

version of the dopamine waveform is applied at 100 Hz to reduce the amount of dopamine adsorbed to the electrode. Second, the electrode potential remains constant (typically at −0.4 V) during a defined holding period to allow for new dopamine adsorption to occur. Third, the waveform is then reapplied to oxidize the dopamine accumulated on the surface. The nonfaradaic current generated during this step is removed through deconvolution techniques using an electrode response function determined in a buffer solution. Subsequent integration of peak oxidation currents is used to calculate the concentration of dopamine in the solution. This technique provides a limit of detection (<10 nM dopamine) sufficient for in vivo use and can be alternated with normal FSCV measurements to monitor rapid dopamine changes at the same microelectrode. An initial study employing FSCAV in the mouse striatum reported basal dopamine levels to be close to 100 nM (98), a value consistent with the concentration range suggested by past studies (8, 91–94).

5.1.2. Ultrafast microdialysis—Recent work (99–101), largely led by the Kennedy group, has led to the realization of the first ultrafast microdialysis techniques. The temporal resolution of micro-dialysis is largely determined by the mass limits of the detection method: High limits require the collection of a larger volume of dialysate and, in turn, longer sampling times. Therefore, coupling microdialysis to analysis techniques with high mass sensitivity, such as capillary electrophoresis with laser-induced fluorescence detection, greatly increases the sampling speed (99–101). Band broadening of the sample via Taylor dispersion during transport limits further improvements in temporal resolution. Wang et al. (102) demonstrated that a segmented flow system significantly reduces the effects of Taylor dispersion. In their setup, segmented flow is accomplished on an integrated polydimethylsiloxane chip positioned at the probe outlet, which mixes the dialysate with fluorogenic reagents for derivatization and introduces an immiscible oil droplet to partition the dialysate into discrete nanoliter fractions. This partitioning prevents the fractions from mixing, thereby preserving temporal information, even when samples are stored for offline analysis. Online analysis with a microfluidic capillary electrophoresis chip demonstrated that this system can provide a temporal resolution of 2 s and is suitable for in vivo amino acid measurements (103).

The segmented flow strategy has also been coupled to low-flow push-pull perfusion to provide fast neurochemical sampling with higher spatial resolution, as sampling occurs only at the tips of two adjoined capillaries (Figure 2) (104). During sampling, a physiological buffer is infused through one capillary (push) while fluid is withdrawn through the second capillary (pull) at an equal flow rate. Given the low flow rates (~50 nL/min), which are used to prevent tissue damage, the sampling of this technique is typically very slow. However, endeavors to couple push-pull perfusion to the segmented flow system have produced results suggesting that subsecond time resolution may be possible. Application of this device in the rat striatum established that this sampling technique could follow glutamate changes with 7-s time resolution and with an 80-fold increase in spatial resolution over conventional microdialysis probes (104).

5.2. Multimodal Measurements

Soon after the introduction of in vivo electrochemical techniques, Millar and colleagues (105–107) realized that a complete understanding of neuronal communication requires knowledge of neurochemical release dynamics and the resulting postsynaptic cell responses. In turn, they developed a method in which catecholamine release and the firing rates of single neurons or units could be monitored at a carbon-fiber microelectrode. In this method, the potential of the electrode is floated between FSCV scans to detect changes in the extracellular potential caused by cell firing (105–107).

When the combined electrochemical/electrophysiological (echem/ephys) method is coupled to iontophoresis, the receptors linking pre- and postsynaptic activity may be identified through pharmacological manipulation (108). Iontophoresis is a classic drug delivery tool using electrophoretic and electroosmotic forces so that an applied current induces the flow of solution through a pulled glass capillary (109). During echem/ephys measurements, the carbon-fiber microelectrode is housed in one capillary of a pulled multibarrel glass assembly. The other barrels contain drug solutions whose dispersions are controlled by a constant-current source. Iontophoresis of electroactive species, such as dopamine, is voltammetrically detected at the carbon fiber to determine the ejected concentration. Iontophoresis of nonelectroactive drugs is indirectly monitored through the addition of a biologically inert, electroactive marker (110). To obtain an approximation of the drug introduced, capillary electrophoresis is used to determine the transport of the drug relative to the marker.

First employed more than 30 years ago, this powerful tool set has only recently been miniaturized for application in awake animals (111). On the miniaturized headstage, a surface-mounted dual-operational amplifier chip provides voltage-follower (electrophysiological) and current-transducer (electrochemical) modes, which are controlled by a CMOS switch. During combined echem/ephys experiments, a triangular waveform scanning between −0.4 V and +1.3 V at 400 V/s is used to detect dopamine changes. This waveform is applied at 5 Hz, half the normal frequency, to provide ~180 ms of electrophysiological recording between scans. Digital time stamps are used to align these measurements with behavioral and iontophoretic events during data analysis. The basic setup for the combined echem/ephys system is shown in Figure 3. Detailed descriptions of the hardware and software components of the combined technique have been published elsewhere (111, 112).

Recent work with this setup has provided new insight into the role of dopamine signaling in the nucleus accumbens (NAc), a brain region mediating motivated behaviors. Operant paradigms such as self-administration and intracranial self-stimulation (ICSS) are used to investigate the physiological and psychological mechanisms guiding reward-seeking behaviors. During such paradigms, the animal learns to complete a task such as pressing a lever to receive a reinforcer (i.e., a reward). In self-administration, the reinforcer is a drug of abuse. In ICSS, the animal receives a rewarding electrical brain stimulation, typically targeting dopaminergic processes. Dopamine is widely implicated in the reinforcing components of psychostimulants and ICSS, but the extent of its neuromodulatory role during such behaviors has been debated (113–116).

The combined echem/ephys technique demonstrates that the medium spiny neurons (MSNs) of the NAc show patterned responses to reward prediction and presentation during ICSS and cocaine self-administration (30, 117). The magnitude of these phasic firing activities tracks with the amount of dopamine release detected, whereas locations with unresponsive cells exhibit no measurable dopamine release. These data provide strong correlation between reward-evoked dopamine and unit responsivity, but initial pharmacological investigations have systemically found that dopamine receptor activation plays little part in generating the MSN firing responses observed during ICSS (118). In another study, microinfusion and iontophoresis were used to apply the drug directly into the NAc, resulting in blocked dopamine receptors (117). With both drug delivery methods, dopamine D1 receptor antagonist SCH23390 blocks lever pressing during ICSS. However, unlike microinfusion, the smaller drug volumes introduced by iontophoresis (119) do not affect animal performance during the task, thereby allowing the neurochemical basis of the behavior to be investigated without influencing behavior.

A more recent study found intriguing differences in the immediate and long-term effects of dopamine receptor modulation in conscious animals at rest (108). Dopamine D1 (SCH 23390) and D2 (raclopride) receptor inhibitors were introduced into the NAc in 15-s ejections, during which only a small number of MSNs were affected. In contrast, long-term analysis found that the baseline firing rates of most cells were either inhibited by D1 or excited by D2 antagonism, consistent with previous literature findings from brain slices. Interestingly, dopamine could evoke immediate cell responses during electrical stimulation when nonelectroactive species such as glutamate are also released. This highlights the role of dopamine as a neuromodulator as opposed to a classical neurotransmitter. Though not directly inhibitory or excitatory, dopamine can have various effects on the overall excitability of MSNs in the NAc and can regulate the immediate actions of glutamate in a receptor-dependent manner.

Use of the combined echem/ephys technique in awake animals is only in its infancy. However, these early results demonstrate the utility of such measurements in delineating the postsynaptic consequences of rapid neurotransmission. Future addition of iontophoresis to this setup will provide a unique opportunity to probe the receptor-based underpinnings of behavior at the local-circuit level.

5.3. Neurotransmitter Detection in Nonrodent Models

Most in vivo electrochemical studies have been conducted in rats, mice, and, to a lesser extent, guinea pigs. This work has provided a great deal of our current knowledge regarding dopamine regulation in the striatum. Unfortunately, the translatability of this information to other species, particularly humans, is tentative. This limitation has spurred attempts to expand electrochemical techniques to nonrodent species. However, as a result of several technological and anatomical challenges, these endeavors have had varying degrees of success. Here we discuss efforts to apply electrochemical neurotransmitter detection in the fly nervous system and in the primate brain.

5.3.1. *Drosophila* (fruit flies)—*Drosophila melanogaster*, more commonly known as the fruit fly, is a valuable model organism. Its short life span, its rapid reproduction cycle, and the ease with which its genetic makeup may be manipulated (120) allow researchers to produce and screen genetic mutations in a matter of months. By contrast, similar manipulations would require years in the rat. Although the *Drosophila* nervous system is composed of only 100,000 neurons (121), it exhibits a notable degree of genetic homology to vertebrates and supports learning and memory (122). Additionally, many of the same monoamine neurotransmitters, including dopamine and serotonin, that *Drosophila* employs are similar to those employed by vertebrates (123). *Drosophila*'s simplicity and genetic flexibility make it an ideal platform to investigate the genetic foundations of neurotransmission.

The size of the *Drosophila* central nervous system (~100 μM across), which is smaller than conventional microdialysis probes, has been the main hindrance in studies of neurotransmitter release. As a result, most neurotransmitter work has involved content analysis of homogenized tissue preparations. Although microelectrodes are well suited to probe biological microenvironments, voltammetric detection of neurotransmission in *Drosophila* has presented additional challenges. For example, the size of the tissue provides very little opportunity to target discrete structures containing only a single, known electroactive neurotransmitter, as is possible in the rat brain. A larger question was how to elicit selective neurotransmitter release when the *Drosophila* nervous system is smaller than commercially available stimulating electrodes.

Owing to such issues, many FSCV measurements conducted in *Drosophila* have involved the application of exogenous dopamine to study the function of the dopamine transporter (124–126). In these experiments, a live fly is immobilized in physiological buffer and dissected to expose its central nervous system. Fluorescent signals produced by GFP-transfected dopamine neurons subsequently guide electrode placement. Pressure ejection through a capillary positioned next to the microelectrode then introduces dopamine, and signal decay is related to the rate of removal by the dopamine transporter. This work has demonstrated that uptake of dopamine from the extracellular space is regulated by similar mechanisms in *Drosophila* and in mammalian species. It has also described an initial protocol for electrochemical measurements in fly preparations.

Study of endogenous monoamine release in *Drosophila* has been accomplished through optogenetic stimulation strategies. Venton and coworkers (127–130) transfected selected groups of monoamine neurons in *Drosophila* to express channelrhodopsin-2 (ChR2), a blue-light-sensitive ion channel. The ion fluxes generated by blue-light exposure cause electrical excitation only in ChR2-expressing cells and, therefore, can be used as a means of selective neuronal activation. Preliminary FSCV studies have proven that blue-light stimulation of ChR2-expressing serotonin and dopamine neurons can elicit measurable release in the ventral nerve cord of *Drosophila* larva and that these monoamine systems have regulatory and frequency-response characteristics comparable with those of the rat brain (127–130).

5.3.2. Nonhuman primates—Given their genetic semblance to humans and their sophisticated cognitive abilities, nonhuman primates are the most clinically relevant animal

models. Though rodent studies have provided most of the insight into human behavior and disease, there is substantial reason to believe that the complexities of primate neurochemistry cannot be fully appreciated through such work. For instance, only in primates is the striatum, a dopamine-dense brain region, anatomically separated into the caudate and putamen by a structure known as the internal capsule. Compared with rodents, primates are also more susceptible to Parkinsonian-like disorders (131, 132), which are mediated in part by dopamine signaling in striatal regions (133).

Given these anatomical and physiological differences, FSCV recordings in primate brain slices have indicated greater complexity in dopamine release and regulation (133–135). Using marmoset striatal slices, Cragg et al. (133–135) observed that, owing to differences in innervation density, dopamine overflow and tissue content were 2–3-fold larger than concentrations found in rodents. Moreover, the magnitude of dopamine release and the rate of its uptake vary significantly among striatal subregions, a characteristic that is not apparent in rodent striata. Interestingly, the rate of dopamine uptake was highest in the dorsal lateral putamen, the area of the striatum most affected by Parkinson's disease. The uptake rate in this region was also two times faster than that reported for rodents, suggesting that the dopamine transporter may contribute to primate susceptibility to Parkinson's disease.

In contrast to the success of brain-slice experiments, application of electrochemical techniques to intact primate brains has progressed slowly since the first attempt in 1981 (136). A handful of studies using amperometric measurements have recorded increased oxidation signals in the monkey striatum with local chemical stimulation, electrical stimulation of dopamine axons, natural reward, and reward prediction (136–138). These data accord with recorded dopamine responses in the rodent brain during such stimuli. However, as amperometry provides very little chemical information, none of the studies was able to verify that the signal was dopaminergic in origin.

In 1998, Earl et al. (139) conducted the first study clearly demonstrating electrochemical detection of dopamine release in the striatum of an anesthetized primate. Using FSCV at a conventional carbon-fiber microelectrode, they measured electrically stimulated dopamine release in the striatum of untreated and 1-methyl-4-phenyl-1,2,3,6-tetrahydropyridine (MPTP)-treated marmosets. MPTP is a neurotoxin that generates Parkinsonian-like degeneration of dopamine neurons. As in rodents, dopamine release in the monkey striatum is dependent on stimulation frequency and is regulated by its autoreceptor and transporter. Moreover, these authors found that dopamine release in MPTP marmosets did not respond to transporter inhibition, consistent with Cragg's later work proposing its involvement in Parkinson's disease.

However, the marmoset is among the smallest primates used in research; similar to the rat, it weighs only 400 g at adulthood (140). Thus, endeavors to employ FSCV in the rhesus monkey, which reaches more than 5,000 g at adulthood (141), are more relevant to the human brain. To probe the rhesus striatum, the electrode must be long enough to hit target regions centimeters, rather than millimeters, beneath the skull. This generates issues regarding not only electrode durability but also fiber resistance, and requires that the conducting wire form a connection to the carbon fiber near the electrode tip. Another set of

concerns arises from the more diffuse distribution of dopamine cells, projections, and terminals in larger animals. As a result, positioning the microelectrode near striatal dopamine terminals becomes a greater challenge.

Accordingly, an FSCV study by our group in collaboration with the Schultz lab detected little dopamine release during recordings in the brain of an awake rhesus monkey (142). The animals were trained in a Pavlovian task where a visual cue predicted the availability of a sweetened liquid, a behavior that involves dopamine neurotransmission. During the behavior, extracellular oxygen and pH fluctuations, which are hemodynamic and metabolic markers of neuronal activity (18, 143), were detected electrochemically. Dopamine-like cyclic voltammograms were also detected at some recording locations, but they were difficult to resolve from the larger oxygen and pH signals.

A more recent FSCV study by Schluter and coworkers (144) explored the use of electrical stimulation to evoke dopamine release in the rhesus striatum. Electrical stimulation of midbrain dopamine neurons in the substantia nigra/ventral tegmental area (SN/VTA) is widely used in rodent studies as an aid in electrode positioning and to study the regulation of dopamine overflow. However, electrical stimulation of the SN/VTA was not an effective means of evoking dopamine release in the rhesus striatum, as the area activated by conventionally sized stimulating electrodes comprises only a small portion of SN/VTA neurons. Increasing the current in attempt to recruit a larger population of neurons resulted in undesirable motor responses that interfered with the recordings. However, local terminal stimulation, a technique regularly used in brain-slice studies, elicited dopamine release in 10 out of 14 attempts and facilitated the recording of dopamine release during an unexpected juice reward. Thus, in agreement with our published work in monkeys, Schluter et al. (144) concluded that dopamine release is more difficult to detect in the primate brain than in rodents.

5.3.3. Humans—To date, endeavors to apply FSCV to the human brain have been made in parallel with deep brain stimulation (DBS) treatment, a type of functional brain surgery that can ameliorate the symptoms of Parkinson’s and other neurological diseases (145–147). The neuronal mechanisms underlying the efficacy of DBS are still largely unknown, though a range of neurotransmitters, including dopamine, serotonin, and adenosine, have been implicated in producing its effects (148, 149). Thus, electrochemical detection of these species during DBS surgery may provide valuable information in the development of new and more effective therapeutics.

Voltammetric recordings from the human brain have employed single fused-silica-based micro-electrode assemblies (Figure 4) (150), housing both the reference and working electrodes to con-fine the damage incurred during implantation. In practice, these probes are positioned near the target of DBS stimulation to eliminate the need for additional surgery. In 2011, the first successful recording from a human used a microelectrode assembly positioned within the striatum. During the procedure, the patient was asked to perform a decision-making task involving monetary investment during which dopamine fluctuations were successfully recorded with FSCV. Thereafter, separate efforts at the Mayo Clinic have created an electrochemical telemetry system called WINCS (wireless instantaneous

neurotransmitter concentration sensing) that is compatible with FSCV or amperometric measurements in humans (151). With the WINCS system, cyclic voltammograms consistent with adenosine release have been recorded in the human thalamus during a treatment for essential tremor (152). Notably, both reports found no adverse effects in patient health or in the efficacy of DBS treatment. The demonstrated safety of electrochemical recordings is a crucial precedent for future clinical studies.

6. CONCLUDING REMARKS

Since Adams' pioneering work more than 40 years ago, the field of in vivo electrochemistry has undergone a great deal of development and standardization. Today, electrochemical techniques are used routinely for high-speed, spatially resolved neurochemical measurements in a number of biological preparations. Although current methods are robust, versatile, and suitable for use by nonelectrochemists, ongoing innovations in sensor design and experimental methodology present exciting new avenues for electrochemical measurements in neuroscience. Future research may provide unprecedented insight into the neurochemical basis of behavior and disease.

Acknowledgments

This research was supported by the National Institutes of Health (DA010900, NS015841, and DA032530).

LITERATURE CITED

1. Janezic S, Threlfell S, Dodson PD, Dowie MJ, Taylor TN, et al. Deficits in dopaminergic transmission precede neuron loss and dysfunction in a new Parkinson model. PNAS. 2013; 110:E4016–25.
2. Koob GF. Addiction is a reward deficit and stress surfeit disorder. Front Psychiatry. 2013; 4:72. [PubMed: 23914176]
3. Weinshenker D. Functional consequences of locus coeruleus degeneration in Alzheimer's disease. Curr Alzheimer Res. 2008; 5:342–45.
4. Jacobsen JP, Medvedev IO, Caron MG. The 5-HT deficiency theory of depression: perspectives from a naturalistic 5-HT deficiency model, the tryptophan hydroxylase $2^{Arg}439^{His}$ knockin mouse. Philos Trans R Soc B. 2012; 367:2444–59.
5. Adams RN. Probing brain chemistry with electroanalytical techniques. Anal Chem. 1976; 48:1126A–38A.
6. Kissinger PT, Hart JB, Adams RN. Voltammetry in brain tissue: a new neurophysiological measurement. Brain Res. 1973; 55:209–13. [PubMed: 4145914]
7. Justice, JB., editor. Voltammetry in the Neurosciences. Clifton, NJ: Humana; 1987.
8. Kawagoe KT, Garris PA, Wiedemann DJ, Wightman RM. Regulation of transient dopamine concentration gradients in the microenvironment surrounding nerve terminals in the rat striatum. Neuroscience. 1992; 51:55–64. [PubMed: 1465186]
9. Robinson DL, Hermans A, Seipel AT, Wightman RM. Monitoring rapid chemical communication in the brain. Chem Rev. 2008; 108:2554–84. [PubMed: 18576692]
10. Mosharov EV, Sulzer D. Analysis of exocytotic events recorded by amperometry. Nat Methods. 2005; 2:651–58. [PubMed: 16118635]
11. Mellander LJ, Trouillon R, Svensson MI, Ewing AG. Amperometric post spike feet reveal most exocytosis is via extended kiss-and-run fusion. Sci Rep. 2012; 2:907. [PubMed: 23205269]
12. Petrovic J, Walsh PL, Thornley KT, Miller CE, Wightman RM. Real-time monitoring of chemical transmission in slices of the murine adrenal gland. Endocrinology. 2010; 151:1773–83. [PubMed: 20181796]

13. Westerink RH, Ewing AG. The PC12 cell as model for neurosecretion. Acta Physiol. 2008; 192:273–85.
14. Manning BM, Hebbel RP, Gupta K, Haynes CL. Carbon-fiber microelectrode amperometry reveals sickle-cell-induced inflammation and chronic morphine effects on single mast cells. ACS Chem Biol. 2012; 7:543–51. [PubMed: 22217155]
15. Borisovska M, Bensen AL, Chong G, Westbrook GL. Distinct modes of dopamine and GABA release in a dual transmitter neuron. J Neurosci. 2013; 33:1790–96. [PubMed: 23365218]
16. Pothos EN. Regulation of dopamine quantal size in midbrain and hippocampal neurons. Behav Brain Res. 2002; 130:203–7. [PubMed: 11864736]
17. Park J, Takmakov P, Wightman RM. In vivo comparison of norepinephrine and dopamine release in rat brain by simultaneous measurements with fast-scan cyclic voltammetry. J Neurochem. 2011; 119:932–44. [PubMed: 21933188]
18. Venton BJ, Michael DJ, Wightman RM. Correlation of local changes in extracellular oxygen and pH that accompany dopaminergic terminal activity in the rat caudate-putamen. J Neurochem. 2003; 84:373–81. [PubMed: 12558999]
19. Bunin MA, Prioleau C, Mailman RB, Wightman RM. Release and uptake rates of 5-hydroxytryptamine in the dorsal raphe and substantia nigra reticulata of the rat brain. J Neurochem. 1998; 70:1077–87. [PubMed: 9489728]
20. Wightman RM, Zimmerman JB. Control of dopamine extracellular concentration in rat striatum by impulse flow and uptake. Brain Res Brain Res Rev. 1990; 15:135–44. [PubMed: 2282449]
21. Wightman RM, Amatore C, Engstrom RC, Hale PD, Kristensen EW, et al. Real-time characterization of dopamine overflow and uptake in the rat striatum. Neuroscience. 1988; 25:513–23. [PubMed: 3399057]
22. McElligott ZA, Fox ME, Walsh PL, Urban DJ, Ferrel MS, et al. Noradrenergic synaptic function in the bed nucleus of the stria terminalis varies in animal models of anxiety and addiction. Neuropsychopharmacology. 2013; 38:1665–73. [PubMed: 23467277]
23. Hashemi P, Dankoski EC, Lama R, Wood KM, Takmakov P, Wightman RM. Brain dopamine and serotonin differ in regulation and its consequences. PNAS. 2012; 109:11510–15. [PubMed: 22778401]
24. Calipari ES, Ferris MJ, Jones SR. Extended access of cocaine self-administration results in tolerance to the dopamine-elevating and locomotor-stimulating effects of cocaine. J Neurochem. 2014; 128:224–32. [PubMed: 24102293]
25. Bergstrom BP, Sanberg SG, Andersson M, Mithyantha J, Carroll FI, Garris PA. Functional reorganization of the presynaptic dopaminergic terminal in parkinsonism. Neuroscience. 2011; 193:310–22. [PubMed: 21787843]
26. Riday TT, Dankoski EC, Krouse MC, Fish EW, Walsh PL, et al. Pathway-specific dopaminergic deficits in a mouse model of Angelman syndrome. J Clin Investig. 2012; 122:4544–54. [PubMed: 23143301]
27. Owesson-White CA, Cheer JF, Beyene M, Carelli RM, Wightman RM. Dynamic changes in accumbens dopamine correlate with learning during intracranial self-stimulation. PNAS. 2008; 105:11957–62. [PubMed: 18689678]
28. Carelli RM. Nucleus accumbens cell firing and rapid dopamine signaling during goal-directed behaviors in rats. Neuropharmacology. 2004; 47(Suppl 1):180–89. [PubMed: 15464136]
29. Addy NA, Daberkow DP, Ford JN, Garris PA, Wightman RM. Sensitization of rapid dopamine signaling in the nucleus accumbens core and shell after repeated cocaine in rats. J Neurophysiol. 2010; 104:922–31. [PubMed: 20554845]
30. Owesson-White CA, Ariansen J, Stuber GD, Cleaveland NA, Cheer JF, et al. Neural encoding of cocaine-seeking behavior is coincident with phasic dopamine release in the accumbens core and shell. Eur J Neurosci. 2009; 30:1117–27. [PubMed: 19735286]
31. Ehrich JM, Phillips PE, Chavkin C. Kappa opioid receptor activation potentiates the cocaine-induced increase in evoked dopamine release recorded in vivo in the mouse nucleus accumbens. Neuropsychopharmacology. 2014; 39:3036–48. [PubMed: 24971603]

32. Park J, Bucher ES, Fontillas K, Owesson-White C, Ariansen JL, et al. Opposing catecholamine changes in the bed nucleus of the stria terminalis during intracranial self-stimulation and its extinction. Biol Psychiatry. 2013; 74:69–76. [PubMed: 23260335]
33. Park J, Kile BM, Wightman RM. In vivo voltammetric monitoring of norepinephrine release in the rat ventral bed nucleus of the stria terminalis and anteroventral thalamic nucleus. Eur J Neurosci. 2009; 30:2121–33. [PubMed: 20128849]
34. Dankoski EC, Agster KL, Fox ME, Moy SS, Wightman RM. Facilitation of serotonin signaling by SSRIs is attenuated by social isolation. Neuropsychopharmacology. 2014; 39:2928–37. [PubMed: 24981046]
35. Hashemi P, Dankoski EC, Petrovic J, Keithley RB, Wightman RM. Voltammetric detection of 5-hydroxytryptamine release in the rat brain. Anal Chem. 2009; 81:9462–71. [PubMed: 19827792]
36. Wilson GS, Johnson MA. In-vivo electrochemistry: What can we learn about living systems? Chem Rev. 2008; 108:2462–81. [PubMed: 18558752]
37. Kiyatkin EA, Wakabayashi KT, Lenoir M. Physiological fluctuations in brain temperature as a factor affecting electrochemical evaluations of extracellular glutamate and glucose in behavioral experiments. ACS Chem Neurosci. 2013; 4:652–65. [PubMed: 23448428]
38. Kiyatkin EA, Lenoir M. Rapid fluctuations in extracellular brain glucose levels induced by natural arousing stimuli and intravenous cocaine: fueling the brain during neural activation. J Neurophysiol. 2012; 108:1669–84. [PubMed: 22723672]
39. Oldenziel WH, Westerink BH. Improving glutamate microsensors by optimizing the composition of the redox hydrogel. Anal Chem. 2005; 77:5520–28. [PubMed: 16131061]
40. Sarter M, Parikh V, Howe WM. Phasic acetylcholine release and the volume transmission hypothesis: time to move on. Nat Rev Neurosci. 2009; 10:383–90. [PubMed: 19377503]
41. Parikh V, Pomerleau F, Huettl P, Gerhardt GA, Sarter M, Bruno JP. Rapid assessment of in vivo cholinergic transmission by amperometric detection of changes in extracellular choline levels. Eur J Neurosci. 2004; 20:1545–54. [PubMed: 15355321]
42. Schmitt LI, Sims RE, Dale N, Haydon PG. Wakefulness affects synaptic and network activity by increasing extracellular astrocyte-derived adenosine. J Neurosci. 2012; 32:4417–25. [PubMed: 22457491]
43. Sanford AL, Morton SW, Whitehouse KL, Oara HM, Lugo-Morales LZ, et al. Voltammetric detection of hydrogen peroxide at carbon fiber microelectrodes. Anal Chem. 2010; 82:5205–10. [PubMed: 20503997]
44. Lugo-Morales LZ, Loziuk PL, Corder AK, Toups JV, Roberts JG, et al. Enzyme-modified carbon-fiber microelectrode for the quantification of dynamic fluctuations of nonelectroactive analytes using fast-scan cyclic voltammetry. Anal Chem. 2013; 85:8780–86. [PubMed: 23919631]
45. Cunha RA. Adenosine as a neuromodulator and as a homeostatic regulator in the nervous system: different roles, different sources and different receptors. Neurochem Int. 2001; 38:107–25. [PubMed: 11137880]
46. Swamy BE, Venton BJ. Subsecond detection of physiological adenosine concentrations using fast-scan cyclic voltammetry. Anal Chem. 2007; 79:744–50. [PubMed: 17222045]
47. Street SE, Walsh PL, Sowa NA, Taylor-Blake B, Guillot TS, et al. PAP and NT5E inhibit nociceptive neurotransmission by rapidly hydrolyzing nucleotides to adenosine. Mol Pain. 2011; 7:80. [PubMed: 22011440]
48. Street SE, Kramer NJ, Walsh PL, Taylor-Blake B, Yadav MC, et al. Tissue-nonspecific alkaline phosphatase acts redundantly with PAP and NT5E to generate adenosine in the dorsal spinal cord. J Neurosci. 2013; 33:11314–22. [PubMed: 23825434]
49. Pajski ML, Venton BJ. The mechanism of electrically stimulated adenosine release varies by brain region. Purinergic Signal. 2013; 9:167–74. [PubMed: 23192278]
50. Pajski ML, Venton BJ. Adenosine release evoked by short electrical stimulations in striatal brain slices is primarily activity dependent. ACS Chem Neurosci. 2010; 1:775–87. [PubMed: 21218131]
51. Cechova S, Venton BJ. Transient adenosine efflux in the rat caudate-putamen. J Neurochem. 2008; 105:1253–63. [PubMed: 18194431]

52. Ross AE, Nguyen MD, Privman E, Venton BJ. Mechanical stimulation evokes rapid increases in extracellular adenosine concentration in the prefrontal cortex. J Neurochem. 2014; 130:50–60. [PubMed: 24606335]
53. Ross AE, Venton BJ. Sawhorse waveform voltammetry for selective detection of adenosine, ATP, and hydrogen peroxide. Anal Chem. 2014; 86:7486–93. [PubMed: 25005825]
54. Glanowska KM, Venton BJ, Moenter SM. Fast scan cyclic voltammetry as a novel method for detection of real-time gonadotropin-releasing hormone release in mouse brain slices. J Neurosci. 2012; 32:14664–69. [PubMed: 23077052]
55. Belchetz PE, Plant TM, Nakai Y, Keogh EJ, Knobil E. Hypophysial responses to continuous and intermittent delivery of hypopthalamic gonadotropin-releasing hormone. Science. 1978; 202:631–33. [PubMed: 100883]
56. Chen P, Moenter SM. GABAergic transmission to gonadotropin-releasing hormone (GnRH) neurons is regulated by GnRH in a concentration-dependent manner engaging multiple signaling pathways. J Neurosci. 2009; 29:9809–18. [PubMed: 19657033]
57. Schmidt AC, Dunaway LE, Roberts JG, McCarty GS, Sombers LA. Multiple scan rate voltammetry for selective quantification of real-time enkephalin dynamics. Anal Chem. 2014; 86:7806–12. [PubMed: 24967837]
58. Bodnar RJ. Endogenous opiates and behavior: 2012. Peptides. 2013; 50:55–95. [PubMed: 24126281]
59. Stamford JA. In vivo voltammetry: prospects for the next decade. Trends Neurosci. 1989; 12:407–12. [PubMed: 2479139]
60. Ponchon JL, Cespuglio R, Gonon F, Jouvet M, Pujol JF. Normal pulse polarography with carbon fiber electrodes for in vitro and in vivo determination of catecholamines. Anal Chem. 1979; 51:1483–86. [PubMed: 484865]
61. Huffman ML, Venton BJ. Carbon-fiber microelectrodes for in vivo applications. Analyst. 2009; 134:18–24. [PubMed: 19082168]
62. Heien ML, Phillips PE, Stuber GD, Seipel AT, Wightman RM. Overoxidation of carbon-fiber microelectrodes enhances dopamine adsorption and increases sensitivity. Analyst. 2003; 128:1413–19. [PubMed: 14737224]
63. Hermans A, Seipel AT, Miller CE, Wightman RM. Carbon-fiber microelectrodes modified with 4-sulfobenzene have increased sensitivity and selectivity for catecholamines. Langmuir. 2006; 22:1964–69. [PubMed: 16489775]
64. Putzbach W, Ronkainen NJ. Immobilization techniques in the fabrication of nanomaterial-based electrochemical biosensors: a review. Sensors. 2013; 13:4811–40. [PubMed: 23580051]
65. Jacobs CB, Peairs MJ, Venton BJ. Review: carbon nanotube based electrochemical sensors for biomolecules. Anal Chim Acta. 2010; 662:105–27. [PubMed: 20171310]
66. Swamy BE, Venton BJ. Carbon nanotube-modified microelectrodes for simultaneous detection of dopamine and serotonin in vivo. Analyst. 2007; 132:876–84. [PubMed: 17710262]
67. Xiao N, Venton BJ. Rapid, sensitive detection of neurotransmitters at microelectrodes modified with self-assembled SWCNT forests. Anal Chem. 2012; 84:7816–22. [PubMed: 22823497]
68. De Volder MF, Tawfick SH, Baughman RH, Hart AJ. Carbon nanotubes: present and future commercial applications. Science. 2013; 339:535–39. [PubMed: 23372006]
69. Zhao J, Zhang X, Di J, Xu G, Yang X, et al. Double-peak mechanical properties of carbon-nanotube fibers. Small. 2010; 6:2612–17. [PubMed: 20941775]
70. Jacobs CB, Ivanov IN, Nguyen MD, Zestos AG, Venton BJ. High temporal resolution measurements of dopamine with carbon nanotube yarn microelectrodes. Anal Chem. 2014; 86:5721–27. [PubMed: 24832571]
71. Schmidt AC, Wang X, Zhu Y, Sombers LA. Carbon nanotube yarn electrodes for enhanced detection of neurotransmitter dynamics in live brain tissue. ACS Nano. 2013; 7:7864–73. [PubMed: 23941323]
72. Zestos AG, Jacobs CB, Trikantzopoulos E, Ross AE, Venton BJ. Polyethyleneimine carbon nanotube fiber electrodes for enhanced detection of neurotransmitters. Anal Chem. 2014; 86:8568–75. [PubMed: 25117550]

73. Swiergiel AH, Palamarchouk VS, Dunn AJ. A new design of carbon fiber microelectrode for in vivo voltammetry using fused silica. J Neurosci Methods. 1997; 73:29–33. [PubMed: 9130675]
74. Gerhardt GA, Ksir C, Pivik C, Dickinson SD, Sabeti J, Zahniser NR. Methodology for coupling local application of dopamine and other chemicals with rapid in vivo electrochemical recordings in freely-moving rats. J Neurosci Methods. 1999; 87:67–76. [PubMed: 10065995]
75. Plotsky P. Probing pathways of neuroendocrine regulation with voltammetric microelectrodes. 1987:273–309. See Ref. 7.
76. Clark JJ, Sandberg SG, Wanat MJ, Gan JO, Horne EA, et al. Chronic microsensors for longitudinal, subsecond dopamine detection in behaving animals. Nat Methods. 2010; 7:126–29. [PubMed: 20037591]
77. Duff A, O'Neill RD. Effect of probe size on the concentration of brain extracellular uric acid monitored with carbon paste electrodes. J Neurochem. 1994; 62:1496–502. [PubMed: 7510782]
78. Kruk ZL, Cheeta S, Milla J, Muscat R, Williams JE, Willner P. Real time measurement of stimulated dopamine release in the conscious rat using fast cyclic voltammetry: Dopamine release is not observed during intracranial self stimulation. J Neurosci Methods. 1998; 79:9–19. [PubMed: 9531455]
79. Wightman RM, Heien ML, Wassum KM, Sombers LA, Aragona BJ, et al. Dopamine release is heterogeneous within microenvironments of the rat nucleus accumbens. Eur J Neurosci. 2007; 26:2046–54. [PubMed: 17868375]
80. Schroeder TJ, Jankowski JA, Senyshyn J, Holz RW, Wightman RM. Zones of exocytotic release on bovine adrenal medullary cells in culture. J Biol Chem. 1994; 269:17215–20. [PubMed: 8006030]
81. Zhang B, Heien ML, Santillo MF, Mellander L, Ewing AG. Temporal resolution in electrochemical imaging on single PC12 cells using amperometry and voltammetry at microelectrode arrays. Anal Chem. 2011; 83:571–77. [PubMed: 21190375]
82. Lin Y, Trouillon R, Svensson MI, Keighron JD, Cans AS, Ewing AG. Carbon-ring microelectrode arrays for electrochemical imaging of single cell exocytosis: fabrication and characterization. Anal Chem. 2012; 84:2949–54. [PubMed: 22339586]
83. Cui HF, Ye JS, Chen Y, Chong SC, Sheu FS. Microelectrode array biochip: tool for in vitro drug screening based on the detection of a drug effect on dopamine release from PC12 cells. Anal Chem. 2006; 78:6347–55. [PubMed: 16970308]
84. Berberian K, Kisler K, Fang Q, Lindau M. Improved surface-patterned platinum microelectrodes for the study of exocytotic events. Anal Chem. 2009; 81:8734–40. [PubMed: 19780579]
85. Carabelli V, Gosso S, Marcantoni A, Xu Y, Colombo E, et al. Nanocrystalline diamond micro-electrode arrays fabricated on sapphire technology for high-time resolution of quantal catecholamine secretion from chromaffin cells. Biosens Bioelectron. 2010; 26:92–98. [PubMed: 20570501]
86. Wang J, Trouillon R, Dunevall J, Ewing AG. Spatial resolution of single-cell exocytosis by microwell-based individually addressable thin film ultramicroelectrode arrays. Anal Chem. 2014; 86:4515–20. [PubMed: 24712854]
87. Wang J, Trouillon R, Lin Y, Svensson MI, Ewing AG. Individually addressable thin-film ultra-microelectrode array for spatial measurements of single vesicle release. Anal Chem. 2013; 85:5600–8. [PubMed: 23627439]
88. Zachek MK, Takmakov P, Park J, Wightman RM, McCarty GS. Simultaneous monitoring of dopamine concentration at spatially different brain locations in vivo. Biosens Bioelectron. 2010; 25:1179–85. [PubMed: 19896822]
89. Zachek MK, Park J, Takmakov P, Wightman RM, McCarty GS. Microfabricated FSCV-compatible microelectrode array for real-time monitoring of heterogeneous dopamine release. Analyst. 2010; 135:1556–63. [PubMed: 20464031]
90. Zhang DA, Rand E, Marsh M, Andrews RJ, Lee KH, et al. Carbon nanofiber electrode for neurochemical monitoring. Mol Neurobiol. 2013; 48:380–85. [PubMed: 23975638]
91. Owesson-White CA, Roitman MF, Sombers LA, Belle AM, Keithley RB, et al. Sources contributing to the average extracellular concentration of dopamine in the nucleus accumbens. J Neurochem. 2012; 121:252–62. [PubMed: 22296263]

92. Kulagina NV, Zigmond MJ, Michael AC. Glutamate regulates the spontaneous and evoked release of dopamine in the rat striatum. Neuroscience. 2001; 102:121–28. [PubMed: 11226675]

93. Borland LM, Michael AC. Voltammetric study of the control of striatal dopamine release by glutamate. J Neurochem. 2004; 91:220–29. [PubMed: 15379902]

94. Chen KC, Budygin EA. Extracting the basal extracellular dopamine concentrations from the evoked responses: re-analysis of the dopamine kinetics. J Neurosci Methods. 2007; 164:27–42. [PubMed: 17498808]

95. Bath BD, Michael DJ, Trafton BJ, Joseph JD, Runnels PL, Wightman RM. Subsecond adsorption and desorption of dopamine at carbon-fiber microelectrodes. Anal Chem. 2000; 72:5994–6002. [PubMed: 11140768]

96. Dengler AK, McCarty GS. Microfabricated microelectrode sensor for measuring background and slowly changing dopamine concentrations. J Electroanal Chem. 2013; 693:28–33.

97. Atcherley CW, Laude ND, Parent KL, Heien ML. Fast-scan controlled-adsorption voltammetry for the quantification of absolute concentrations and adsorption dynamics. Langmuir. 2013; 29:14885–92. [PubMed: 24245864]

98. Atcherley CW, Wood KM, Parent KL, Hashemi P, Heien ML. The coaction of tonic and phasic dopamine dynamics. Chem Commun. 2015; 51:2235–38.

99. Lada MW, Vickroy TW, Kennedy RT. High temporal resolution monitoring of glutamate and aspartate in vivo using microdialysis on-line with capillary electrophoresis with laser-induced fluorescence detection. Anal Chem. 1997; 69:4560–65. [PubMed: 9375517]

100. Hogan BL, Lunte SM, Stobaugh JF, Lunte CE. On-line coupling of in vivo microdialysis sampling with capillary electrophoresis. Anal Chem. 1994; 66:596–602. [PubMed: 8154588]

101. Thompson JE, Vickroy TW, Kennedy RT. Rapid determination of aspartate enantiomers in tissue samples by microdialysis coupled on-line with capillary electrophoresis. Anal Chem. 1999; 71:2379–84. [PubMed: 10405606]

102. Wang M, Roman GT, Schultz K, Jennings C, Kennedy RT. Improved temporal resolution for in vivo microdialysis by using segmented flow. Anal Chem. 2008; 80:5607–15. [PubMed: 18547059]

103. Wang M, Slaney T, Mabrouk O, Kennedy RT. Collection of nanoliter microdialysate fractions in plugs for off-line in vivo chemical monitoring with up to 2 s temporal resolution. J Neurosci Methods. 2010; 190:39–48. [PubMed: 20447417]

104. Slaney TR, Nie J, Hershey ND, Thwar PK, Linderman J, et al. Push-pull perfusion sampling with segmented flow for high temporal and spatial resolution in vivo chemical monitoring. Anal Chem. 2011; 83:5207–13. [PubMed: 21604670]

105. Armstrong-James M, Fox K, Kruk ZL, Millar J. Quantitative ionophoresis of catecholamines using multibarrel carbon fibre microelectrodes. J Neurosci Methods. 1981; 4:385–406. [PubMed: 7321578]

106. Millar J, Barnett TG. Basic instrumentation for fast cyclic voltammetry. J Neurosci Methods. 1988; 25:91–95. [PubMed: 3172827]

107. Stamford JA, Palij P, Davidson C, Jorm CM, Millar J. Simultaneous “real-time” electrochemical and electrophysiological recording in brain slices with a single carbon-fibre microelectrode. J Neurosci Methods. 1993; 50:279–90. [PubMed: 8152239]

108. Belle AM, Owesson-White C, Herr NR, Carelli RM, Wightman RM. Controlled iontophoresis coupled with fast-scan cyclic voltammetry/electrophysiology in awake, freely moving animals. ACS Chem Neurosci. 2013; 4:761–71. [PubMed: 23480099]

109. Herr NR, Wightman RM. Improved techniques for examining rapid dopamine signaling with iontophoresis. Front Biosci. 2013; 5:249–57.

110. Herr NR, Kile BM, Carelli RM, Wightman RM. Electroosmotic flow and its contribution to iontophoretic delivery. Anal Chem. 2008; 80:8635–41. [PubMed: 18947198]

111. Takmakov P, McKinney CJ, Carelli RM, Wightman RM. Instrumentation for fast-scan cyclic voltammetry combined with electrophysiology for behavioral experiments in freely moving animals. Rev Sci Instrum. 2011; 82:074302. [PubMed: 21806203]

112. Bucher ES, Brooks K, Verber MD, Keithley RB, Owesson-White C, et al. Flexible software platform for fast-scan cyclic voltammetry data acquisition and analysis. Anal Chem. 2013; 85:10344–53. [PubMed: 24083898]
113. Murray B, Shizgal P. Evidence implicating both slow- and fast-conducting fibers in the rewarding effect of medial forebrain bundle stimulation. Behav Brain Res. 1994; 63:47–60. [PubMed: 7945977]
114. Hernandez G, Hamdani S, Rajabi H, Conover K, Stewart J, et al. Prolonged rewarding stimulation of the rat medial forebrain bundle: neurochemical and behavioral consequences. Behav Neurosci. 2006; 120:888–904. [PubMed: 16893295]
115. Wise RA. Addictive drugs and brain stimulation reward. Annu Rev Neurosci. 1996; 19:319–40. [PubMed: 8833446]
116. Sunsay C, Rebec GV. Extinction and reinstatement of phasic dopamine signals in the nucleus accumbens core during Pavlovian conditioning. Behav Neurosci. 2014; 128:579–87. [PubMed: 25111335]
117. Cheer JF, Aragona BJ, Heien ML, Seipel AT, Carelli RM, Wightman RM. Coordinated accumbal dopamine release and neural activity drive goal-directed behavior. Neuron. 2007; 54:237–44. [PubMed: 17442245]
118. Cheer JF, Heien ML, Garris PA, Carelli RM, Wightman RM. Simultaneous dopamine and single-unit recordings reveal accumbens GABAergic responses: implications for intracranial self-stimulation. PNAS. 2005; 102:19150–55. [PubMed: 16380429]
119. Kirkpatrick DC, Edwards MA, Flowers PA, Wightman RM. Characterization of solute distribution following iontophoresis from a micropipet. Anal Chem. 2014; 86:9909–16. [PubMed: 25157675]
120. Sang, JH. *Drosophila melanogaster*: the fruit fly. In: Reeve, ECR., editor. Encyclopedia of Genetics. London: Fitzroy Dearborn; 2001. p. 157-62.
121. Ito M, Masuda N, Shinomiya K, Endo K, Ito K. Systematic analysis of neural projections reveals clonal composition of the *Drosophila* brain. Curr Biol. 2013; 23:644–55. [PubMed: 23541729]
122. Sokolowski MB. *Drosophila*: Genetics meets behaviour. Nat Rev Genet. 2001; 2:879–90. [PubMed: 11715043]
123. Monastirioti M. Biogenic amine systems in the fruit fly *Drosophila melanogaster*. Microsc Res Tech. 1999; 45:106–21. [PubMed: 10332728]
124. Berglund EC, Makos MA, Keighron JD, Phan N, Heien ML, Ewing AG. Oral administration of methylphenidate blocks the effect of cocaine on uptake at the *Drosophila* dopamine transporter. ACS Chem Neurosci. 2013; 4:566–74. [PubMed: 23402315]
125. Makos MA, Han KA, Heien ML, Ewing AG. Using in vivo electrochemistry to study the physiological effects of cocaine and other stimulants on the *Drosophila melanogaster* dopamine transporter. ACS Chem Neurosci. 2010; 1:74–83. [PubMed: 20352129]
126. Makos MA, Kim YC, Han KA, Heien ML, Ewing AG. In vivo electrochemical measurements of exogenously applied dopamine in *Drosophila melanogaster*. Anal Chem. 2009; 81:1848–54. [PubMed: 19192966]
127. Xiao N, Privman E, Venton BJ. Optogenetic control of serotonin and dopamine release in *Drosophila* larvae. ACS Chem Neurosci. 2014; 5:666–73. [PubMed: 24849718]
128. Vickrey TL, Condron B, Venton BJ. Detection of endogenous dopamine changes in *Drosophila melanogaster* using fast-scan cyclic voltammetry. Anal Chem. 2009; 81:9306–13. [PubMed: 19842636]
129. Borue X, Cooper S, Hirsh J, Condron B, Venton BJ. Quantitative evaluation of serotonin release and clearance in *Drosophila*. J Neurosci Methods. 2009; 179:300–8. [PubMed: 19428541]
130. Vickrey TL, Venton BJ. *Drosophila* dopamine2-like receptors function as autoreceptors. ACS Chem Neurosci. 2011; 2:723–29. [PubMed: 22308204]
131. Johannessen JN, Chiueh CC, Burns RS, Markey SP. Differences in the metabolism of MPTP in the rodent and primate parallel differences in sensitivity to its neurotoxic effects. Life Sci. 1985; 36:219–24. [PubMed: 3871242]
132. Schober A. Classic toxin-induced animal models of Parkinson's disease: 6-OHDA and MPTP. Cell Tissue Res. 2004; 318:215–24. [PubMed: 15503155]

133. Cragg SJ, Hille CJ, Greenfield SA. Dopamine release and uptake dynamics within nonhuman primate striatum in vitro. J Neurosci. 2000; 20:8209–17. [PubMed: 11050144]

134. Cragg SJ, Hille CJ, Greenfield SA. Functional domains in dorsal striatum of the nonhuman primate are defined by the dynamic behavior of dopamine. J Neurosci. 2002; 22:5705–12. [PubMed: 12097522]

135. Cragg SJ. Variable dopamine release probability and short-term plasticity between functional domains of the primate striatum. J Neurosci. 2003; 23:4378–85. [PubMed: 12764127]

136. Lindsay WS, Herndon JG Jr, Blakely RD, Justice JB Jr, Neill DB. Voltammetric recording from neostriatum of behaving rhesus monkey. Brain Res. 1981; 220:391–96. [PubMed: 7284764]

137. Gerhardt GA, Cass WA, Hudson J, Henson M, Zhang Z, et al. In vivo electrochemical studies of dopamine overflow and clearance in the striatum of normal and MPTP-treated rhesus monkeys. J Neurochem. 1996; 66:579–88. [PubMed: 8592127]

138. Yoshimi K, Naya Y, Mitani N, Kato T, Inoue M, et al. Phasic reward responses in the monkey striatum as detected by voltammetry with diamond microelectrodes. Neurosci Res. 2011; 71:49–62. [PubMed: 21645558]

139. Earl CD, Sautter J, Xie J, Kruk ZL, Kupsch A, Oertel WH. Pharmacological characterisation of dopamine overflow in the striatum of the normal and MPTP-treated common marmoset, studied in vivo using fast cyclic voltammetry, nomifensine and sulpiride. J Neurosci Methods. 1998; 85:201–9. [PubMed: 9874156]

140. Hearn, J. The common marmoset (*Callithrix jacchus*). In: Hearn, J., editor. Reproduction in New World Primates. Netherlands: Springer; 1983. p. 181-215.

141. Grand TI. Body weight: its relation to tissue composition, segment distribution, and motor function II. Development of *Macaca mulatta*. Am J Phys Anthropol. 1977; 47:241–48. [PubMed: 410306]

142. Ariansen JL, Heien ML, Hermans A, Phillips PE, Hernadi I, et al. Monitoring extracellular pH, oxygen, and dopamine during reward delivery in the striatum of primates. Front Behav Neurosci. 2012; 6:36. [PubMed: 22783176]

143. Heales DS. pH and brain function. Brain. 1999; 122:1794–96.

144. Schluter EW, Mitz AR, Cheer JF, Averbeck BB. Real-time dopamine measurement in awake monkeys. PLOS ONE. 2014; 9:e98692. [PubMed: 24921937]

145. Stefurak T, Mikulis D, Mayberg H, Lang AE, Hevenor S, et al. Deep brain stimulation for Parkinson's disease dissociates mood and motor circuits: a functional MRI case study. Mov Disord. 2003; 18:1508–16. [PubMed: 14673888]

146. Sachdev PS, Mohan A, Cannon E, Crawford JD, Silberstein P, et al. Deep brain stimulation of the antero-medial globus pallidus interna for Tourette syndrome. PLOS ONE. 2014; 9:e104926. [PubMed: 25136825]

147. Laxpati NG, Kasoff WS, Gross RE. Deep brain stimulation for the treatment of epilepsy: circuits, targets, and trials. Neurotherapeutics. 2014; 11:508–26. [PubMed: 24957200]

148. Figee M, de Koning P, Klaassen S, Vulink N, Mantione M, et al. Deep brain stimulation induces striatal dopamine release in obsessive-compulsive disorder. Biol Psychiatry. 2014; 75:647–52. [PubMed: 23938318]

149. van Dijk A, Klompmakers AA, Feenstra MG, Denys D. Deep brain stimulation of the accumbens increases dopamine, serotonin, and noradrenaline in the prefrontal cortex. J Neurochem. 2012; 123:897–903. [PubMed: 23061486]

150. Kishida KT, Sandberg SG, Lohrenz T, Comair YG, Saez I, et al. Sub-second dopamine detection in human striatum. PLOS ONE. 2011; 6:e23291. [PubMed: 21829726]

151. Kasasbeh A, Lee K, Bieber A, Bennet K, Chang SY. Wireless neurochemical monitoring in humans. Stereotact Funct Neurosurg. 2013; 91:141–47. [PubMed: 23445903]

152. Chang SY, Kim I, Marsh MP, Jang DP, Hwang SC, et al. Wireless fast-scan cyclic voltammetry to monitor adenosine in patients with essential tremor during deep brain stimulation. Mayo Clin Proc. 2012; 87:760–65. [PubMed: 22809886]

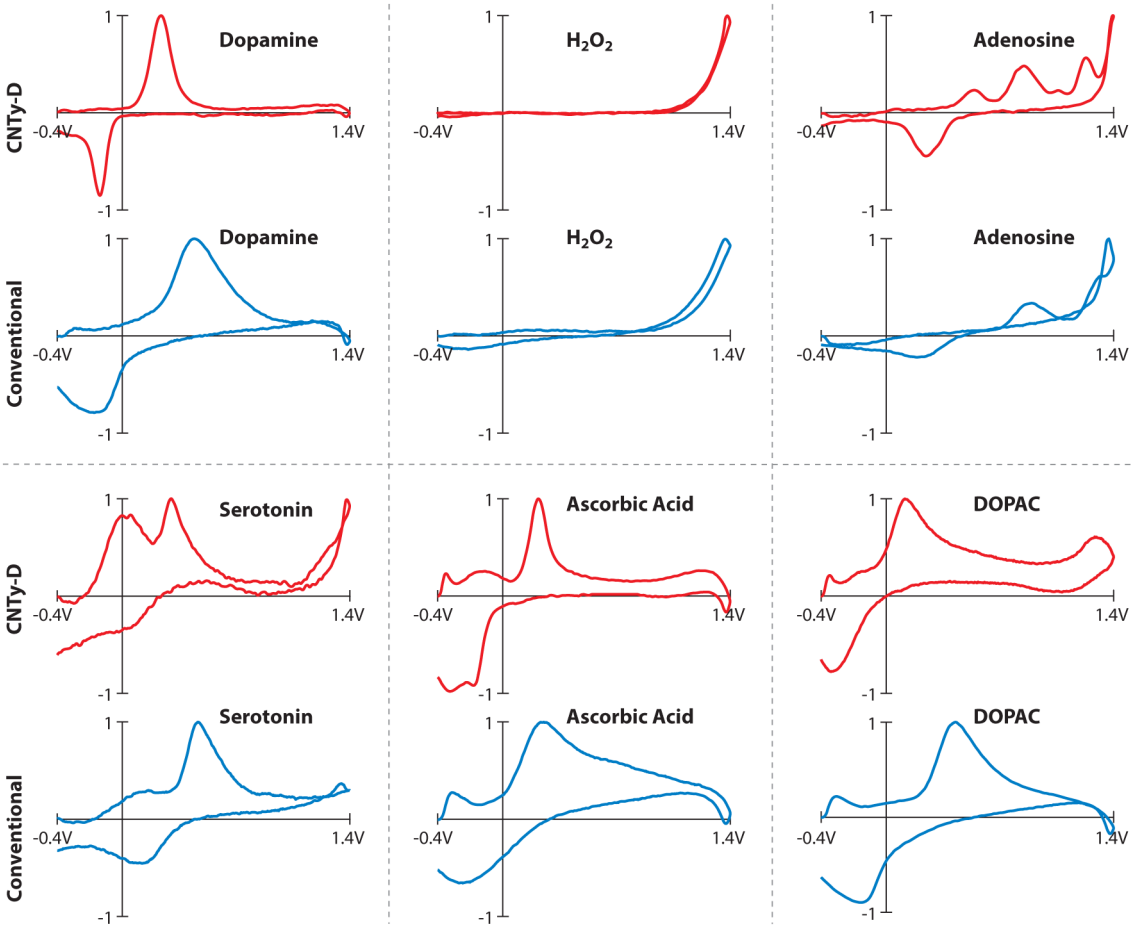

Figure 1.

Voltammograms for several analytes commonly encountered in brain tissue. Data collected using CNTy-D electrodes are shown in red, and those collected using conventional carbon-fiber electrodes are shown in black. Potential was scanned from −0.4 V to +1.4 V and back at 400 V/s and applied at 10 Hz to allow for the detection of many analytes. Currents are normalized to highlight differences in the features of each voltammogram. Figure reprinted with permission from Reference 71. Abbreviations: CNTy-D, carbon-nanotube yarn-disk; DOPAC, 3,4-dihydroxyphenylacetic acid.

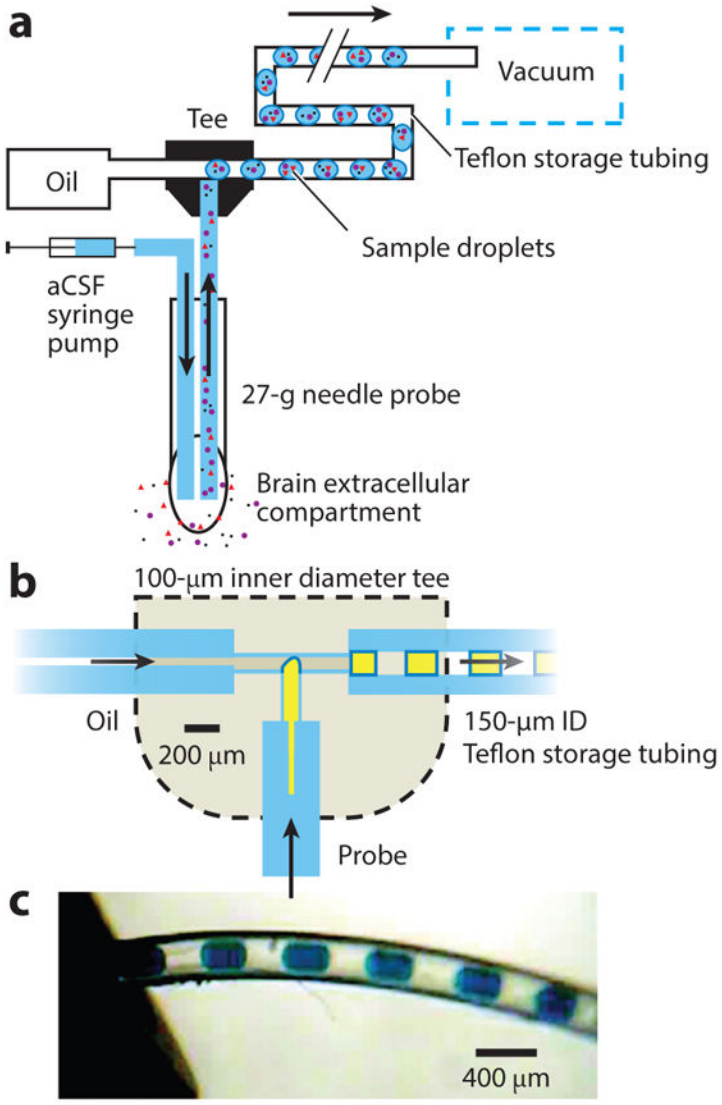

Figure 2.

(*a*) Segmented flow–coupled low-flow push-pull probe. Artificial cerebrospinal fluid (aCSF) is infused directly into the tissue, while extracellular fluid is withdrawn at an equal flow rate. Suction for sampling flow is generated by a vacuum applied to the outlet of the Teflon storage tubing, which also pulls the oil to generate the segmented sample stream. (*b*) Internal tee geometry (tee outline not to scale). (*c*) Photograph of 6-nL sample segments (*blue food dye*) entering the storage tubing at the tee outlet. Figure reprinted with permission from Reference 104.

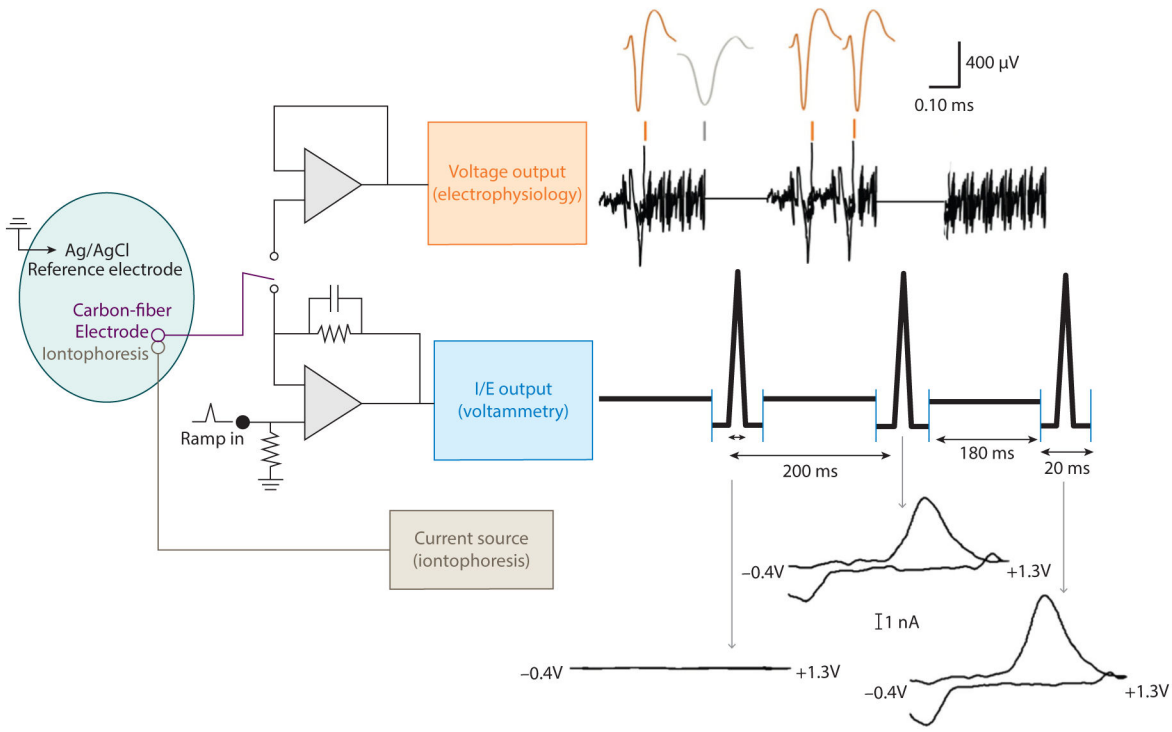

Figure 3.

Electronics and outputs for combined fast-scan cyclic voltammetry/electrophysiology. The same carbon-fiber electrode and reference electrode are used for both circuits, and the reference electrode also serves as ground for the iontophoresis circuit. Output of the carbon-fiber electrode is connected to a voltage follower to monitor cell firing (*upper circuitry*). Every 200 ms, the carbon-fiber microelectrode is switched from the electrophysiology circuit to the lower voltammetry circuitry for 20 ms. In this position, the amplifier controls the electrode potential, and the current is monitored. Synchronized outputs for both circuits are shown to the right of the circuitry. When the lower circuit is completed, the electrode is held at −0.4 V, then over 8.5 ms, it is scanned from −0.4 V to +1.3 V and back to −0.4 V. Changes in current during each scan are indicated with arrows. During this time, no voltage changes are seen in the electrophysiology (when circuit was open but program still recorded data). With the upper circuit connected, changes in voltage were monitored. Colored marks above voltage readout indicate regions of 180 ms that have been expanded above. Voltage signals from medium spiny neurons of interest (*orange spikes*) are separated from signals generated by other cells (*gray spike*) through principal component analysis. Figure adapted with permission from Reference 108.

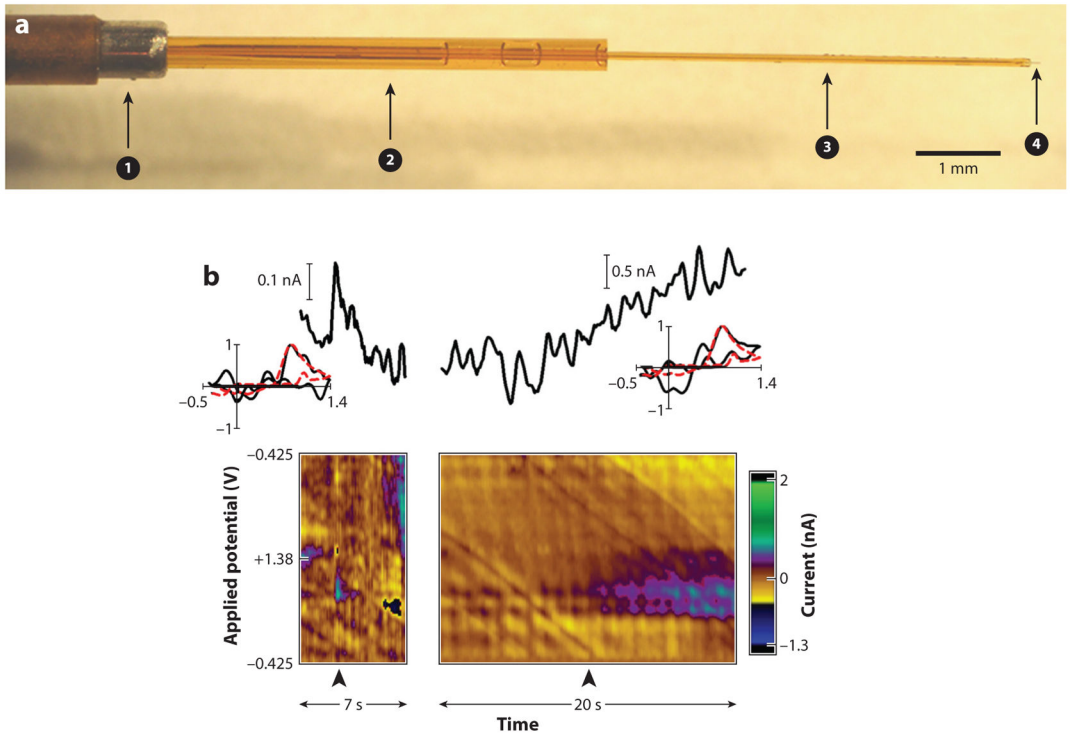

Figure 4.

(*a*) Carbon-fiber microelectrode design for human applications. The electrode is assembled from two polyamide-coated fused silica capillaries and a polyamide-coated stainless steel protective tube. The smaller capillary (*arrow 3*) (90 μm o.d.) houses the carbon fiber (*arrow 4*) and connection wire. Epoxy is used to form a seal at the tip. This smaller capillary is inserted into the larger capillary (*arrow 2*) (360 μm o.d.) so that it protrudes 5 mm from the tip for increased stability. This assembly is then encased at one end with the stainless steel protective tube (*arrow 1*) containing a stainless steel reference electrode. (*b*) Voltammetric signals measured at an electrode implanted in the human caudate: (*left*) subsecond changes and (*right*) changes over several seconds. Changes in electrochemical current are measured at the peak oxidation potential for dopamine (+0.65–0.75 V). Insets show cyclic voltammograms from the patient's brain (*black trace*) compared with a standard reference cyclic voltammogram for dopamine (*dashed red trace*): r2 = 0.75 (*left*), r2 = 0.765 (*right*), and $p < 0.0001$ for both. These cyclic voltammograms were measured at the time points indicated by the black arrowheads in the lower panels, which show two-dimensional plots with electrochemical current: nA indicates pseudo color (see color bar to the right) plotted against time (horizontal axis) and applied potential (vertical axis). Figure adapted with permission from Reference 150.